ACS OMEGA

http://pubs.acs.org/journal/acsodf

Article

Subcritical Hydrothermal Liquefaction as a Pretreatment for Enzymatic Degradation of Polyurethane

Riccardo Gallorini, Benedetta Ciuffi, Feliciana Real Fernández, Cosimo Carozzini, Enrico Ravera, Anna Maria Papini, and Luca Rosi*

Cite This: *ACS Omega* 2022, 7, 37757−37763

Read Online

ACCESS | Metrics & More | Article Recommendations | Supporting Information

ABSTRACT: Enzymatic digestion is a promising alternative in the upconversion of plastic waste compared to traditional chemical recycling methods, because it warrants the use of milder conditions. However, enzymes are hardly able to penetrate the bulk of the plastic material; thus, a pretreatment is necessary to promote the reaction. In this study we investigate hydrothermal liquefaction as a thermal pretreatment of a commercial polyurethane before performing an enzymatic digestion. The feedstock is a rigid polyurethane foam. The structure and chemical composition of the feedstock were analyzed through FTIR analysis and solid-state ^{13}C NMR. The polyurethane was then subjected to hydrothermal liquefaction using either ultrapure water or KOH as a basic catalyst. Enzymatic digestion was then performed on the organic fraction obtained from both experiments using a lipase extracted from *Candida rugosa*. The LC-MS analysis of the digests shows an increase in some signal intensities due to the degradation of oligomeric fragments. This new way of recycling allows the recovery of important chemicals such as quinolines and 4,4′-methylenedianiline. With this study we demonstrate that hydrothermal liquefaction coupled with enzymatic digestion is a suitable alternative for handling polyurethane waste.

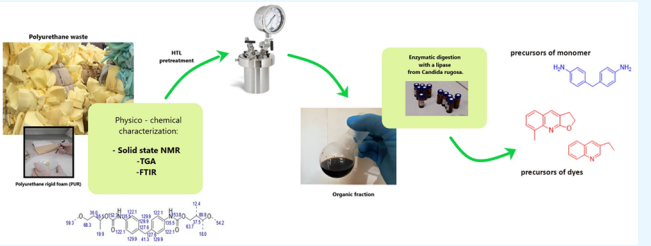

INTRODUCTION

Due to their low cost and versatility, plastics have become ubiquitous materials in the modern economy. The use of plastic products has increased 20-fold in the last half century and is expected to double again in the next 20 years.[1] The European production alone accounts for 55 million tons of plastics produced, representing 15% of world production in 2020.[2] In 2020, 29.5 million tons of postconsumer plastic waste were collected. Of this, more than one-third was recycled, while one-fourth was landfilled.[2] Polyurethane (PU) resins account for 7.8% of the resins produced in 2020, making them the sixth most widely used plastics in the world.[2] The reason for this widespread use of PUs is linked to their strength, durability, and elasticity, which make it possible to use them as replacements for metals, rubber, and other plastics in a wide variety of applications.[3] Rigid PU foams are widely used in construction for thermal and acoustic insulation, while flexible foams are used for cushioning, mattresses, and car interiors. PUs represent a challenge for recycling for a number of reasons. They are thermosetting, which prevents recycling through thermomechanical treatments such as re-extrusion. The main mechanical recycling route for these polymers is rebonding. PU waste, both postindustrial and postconsumer, is shredded and added with a binder (usually a polymeric isocyanate), and after heating (100−200 °C) and compression (30−200 bar), PU waste can be converted into new products.[4] The binder is activated by steam and, after curing, gives the products a high density and resilience, which makes them suitable for damping vibrations and to produce sports flooring.[5] However, chemical conversion to smaller molecules, to be used as precursors in fine chemical synthesis, could prove a more versatile means of recycling.

Enzymatic degradation is emerging as one of the most promising recycling strategies, giving the possibility to obtain high-added-value chemicals from end-of-life polymeric materials through the use of mild reaction conditions.[6] At variance with standard chemical recycling methods, enzymatic processes intrinsically revolve around the use of close-to-physiological conditions, which are milder than standard processes in terms of temperature, pressure, and use of noxious solvents and thus can considerably reduce process costs. The reactions involved occur at the interface between the enzyme-containing solution and the polymer; therefore, these reactions are generally slow because enzymes have an extremely inefficient contact with insoluble substrates such as

Received: July 27, 2022
Accepted: October 6, 2022
Published: October 14, 2022

PU.[7] The process is made even less efficient in the case of commercial products, where hydrophobic sealing agents are added, such as organic silicone, to improve the contact angle, hardness, and impact strength of the polyurethane coating.[8] Due to the high complexity in the polymer structures of PU, an efficient biodegradation at a promising rate has not yet been reported.[9] PUs are particularly recalcitrant not only to enzymatic degradation but also to biodegradation performed by microorganisms, which is generally triggered by external factors such as temperature, humidity, pH, and especially the presence of oxygen, without which biodegradation does not occur.[10] Only certain types of PUs, such as polyester polyurethanes, are biodegraded, whereas polyether polyurethanes are very slow to biodegrade.[11] In this context, the presence of urethane bonds makes polyurethanes susceptible to hydrolysis by enzymes secreted by microorganisms, which can be a suitable alternative to induce PU degradation. One of the microorganisms enabling degradation of these polymers in bulk form is *Aspergillus tubingensis* that, after an incubation time of 27 days, can grow in the presence of the polymer, causing surface changes such as cracking, erosion, and pore formation.[12] On these grounds, we can conclude that pretreatments aimed at increasing the accessibility of urethane bonds are essential to promote the enzymatic degradation of PUs.

Hydrothermal liquefaction (HTL) is a thermochemical process that takes place in the presence of water under sub- or supercritical conditions. Water near its critical point (T_c = 647.3 K, P_c = 22.1 MPa) acts at the same time as a reactant and a solvent, taking part in the depolymerization reactions of plastics. Under these conditions, the properties of water change as compared to those at room temperature (Table S1, Supporting Information), allowing for a precise control of the degree of hydrolysis and solubility of the postprocessing material. HTL is mainly optimized for biomass conversion to obtain bio-oil, an oil with high energy value,[13] but it has been poorly investigated for the treatment of plastics. HTL allows for processing wet feedstocks, thus eliminating the need for drying as a pretreatment, as is necessary for gasification and pyrolysis processes.[14] HTL as an upconversion process is also extremely flexible in terms of feedstock, as it allows for the contemporary conversion of a heterogeneous material (in terms of chemical nature, color, size, and other physical properties) within the same reactor.[15] Polymers with heteroatoms in the main chain, such as PET, PA6, PA66, PC, and PU, are subject to hydrolytic degradation and can be broken down into alcohols, carboxylic acids, amines, or amides as the main products[16,17] as a result of the HTL-induced depolymerization processes.

Through the HTL processing, four distinct phases are always obtained:

(1) a liquid/semisolid organic phase, consisting of organic compounds with low molecular weight, derived from depolymerization reactions
(2) an aqueous phase, with dissolved organic compounds called water-soluble organics (WSO).
(3) a solid phase, formed by unreacted compounds and inorganic and carbonaceous products (char)
(4) a gaseous phase, containing the gases produced during feedstock degradation reactions

The yield of the various fractions changes according to the applied operating conditions: short reaction times favor the yield of oil, while long reaction times increase the yields of char and gas.

We propose that depolymerization by HTL can facilitate enzymatic degradation: performing it on a substrate that has already been subjected to pretreatment is expected to promote the reactions, as the depolymerization by enzymes occurs readily for water-soluble or water-accessible substrates. The aim of this work is valorizing a commercial polyurethane by developing a recycling method for obtaining value-added chemicals. A pretreatment performed by HTL under subcritical conditions followed by enzymatic degradation was carried out on the organic phase, in order to degrade the residual oligomers. This makes the biodegradation of the polymer faster and more efficient.

To the best of our knowledge, this is the first time that the HTL process has been used as a pretreatment for subsequent enzymatic degradation of plastics.

MATERIALS AND METHODS

Feedstock. A white rigid polyurethane foam (PUR), (Figure S1, Supporting Information) used for model making and readily available in specialty DIY stores, was tested in this study. The material was characterized by FTIR and ^{13}C NMR spectroscopy, thermogravimetric analysis, and CHNS elemental analysis. Before undergoing enzymatic digestion, the feedstock was mechanically pulverized.

Experimental Equipment and Procedure. The HTL experiments were carried out in a 160 mL stainless steel Parr autoclave. The heating system consisted of a 1 kW electric band heater regulated by a proportional integral derivative (PID) controller (±1 °C). The autoclave was equipped with a stirrer, a pressure sensor (Parr Model 4842, in which pressure is displayed with 1 psi resolution and 10 psi accuracy), and a J-type thermocouple. Overall, two tests were carried out in duplicate. The operating conditions are reported in Table 1.

Table 1. Reaction Conditions of the Tests

	temp (°C)	reaction time (min)	feedstock mass (g)	water volume (mL)	catalyst (g KOH)
ID1	350	20	3	70	
ID2	350	20	3	70	1.12

For each test, 3 g of PUR was used in combination with 70 mL of total liquid volume, consisting of ultrapure water (0.05 $\mu S\ cm^{-1}$)[18] or ultrapure water + KOH. In test 2 (ID2) the base concentration is equal to 17.2 g/L, in accordance with the literature.[16] This mixture was transferred to the Parr autoclave, which was then closed. Before each experiment, a leakage test over the autoclave with argon at 80 bar was performed. Subsequently, three purging cycles with N_2 (5 bar) were carried out in order to ensure an inert atmosphere. Finally, the autoclave was charged with 6 atm of N_2. In all tests the temperature was set at 350 °C and the average heating rate was 4.7 °C min^{-1}. The reaction temperature was reached in 50 min and was maintained for 20 min. At the end of the reaction, the autoclave was rapidly cooled by immersing it in a bath of water and ice, and the gas was vented out. The aqueous phase containing water-soluble organic compounds (WSO) was separated at the end of the cooling process via centrifugation and decanting. The reactor and its contents were washed with methanol, and then the obtained suspension was filtered under

https://doi.org/10.1021/acsomega.2c04734
ACS Omega 2022, 7, 37757−37763

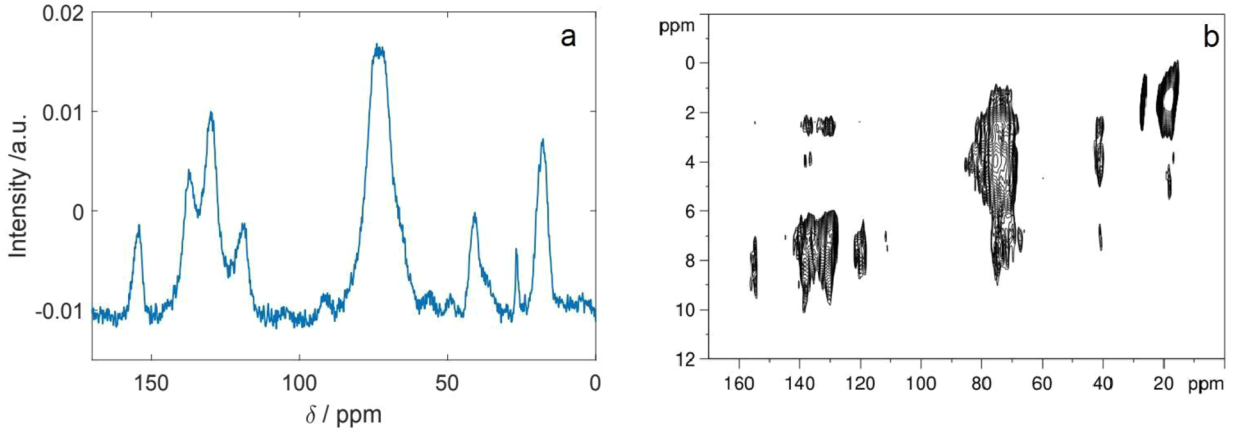

Figure 1. Solid-state ^{13}C NMR spectra: (a) $\{^1H\}^{13}C$ CP; (b) $\{^1H\}^{13}C$ HETCOR.

vacuum over a glass microfiber filter (1 μm). The solid residue was dried overnight at 100 °C. The organic phase (oil) was extracted in methanol and combined with the organic phase from centrifugation of the supernatant.

Determination of the Yield. From each HTL experiment four different fractions were obtained: solid, gas, oil, and aqueous fraction. The yields of each fraction were calculated using eqs 1−4, in which w indicates the weight.

$$\text{solid residue yield (\%)} = \frac{w_{\text{solid}}}{w_{\text{feedstock}}} \times 100 \quad (1)$$

$$\text{oil product yield (\%)} = \frac{w_{\text{oil}}}{w_{\text{feedstock}}} \times 100 \quad (2)$$

The weights of the solid and oil fractions were measured with a balance, while the amount of gas produced during the reactions was determined as the difference between the weight of the reactor before heating and after venting the gaseous products at the end of the cooling process.

$$\text{gas yield (\%)} = \frac{\text{weight after venting} - \text{initial weight before heating}}{w_{\text{feedstock}}} \times 100 \quad (3)$$

Water-soluble organics and unrecovered products (i.e., all losses due to experimental operations) were estimated by difference:

$$\text{WSO + unrecovered (\%)} = 100 - (\text{solid residue yield} + \text{oil product yield} + \text{gas yield}) \quad (4)$$

Enzymatic Digestion. For the study of enzymatic degradation reactions, a lipase extracted from *Candida rugosa* (988 U/mg) was chosen based on the literature.[19] Samples of approximately 30 mg of the polyurethane foam were introduced into two 15 mL polypropylene tubes, in the forms of fragments and a powder, respectively.

A 10 mL portion of an aqueous solution containing the enzyme was then prepared with a total activity of 5000U, in phosphate buffer at pH 7.2.

A 3 mL portion (1500U) of this solution[19] was taken and inserted respectively in test tubes containing the two samples. The tubes were then placed inside an orbital incubator and continuously stirred at 37 °C. After 1 week, 1 mL of the supernatant was removed. The dissolved enzyme was precipitated by adding 10 mL of acetonitrile and subsequently centrifuging at 4 °C and 4000 rpm. The supernatant was separated and concentrated by partial evaporation of the solvent and subsequently analyzed by LC-MS and GC-MS. The same procedure was also subsequently carried out on the oils obtained from HTL, brought to dryness by the respective solutions.

Analytical Methods. *FTIR Spectroscopy.* FTIR spectra of the samples were obtained using a Shimadzu IR Tracer-100 spectrometer, equipped with a QATR 10 Single-Reflection ATR with a Diamond Crystal (Shimadzu, Nishinokyo Kuwabara-cho, Kyoto, JP), operating with a maximum resolution of 0.25 cm^{-1} and a spectral range in the mid-IR region (4100−500 cm^{-1}). The spectra have been acquired in transmittance mode (%) using 45 scans for each sample. Measurements were carried out in triplicate for each sample.

GC-MS. A qualitative analysis of the organic compounds in the oil phase was performed with a GCMS-QP2020 NX instrument (Shimadzu, Nishinokyo Kuwabara-cho, Kyoto, JP), equipped with a SH-Rxi-5 ms column (length 30 m, internal diameter 0.25 mm, film diameter 0.25 μm). The injector temperature was set at 280 °C, while a gradient from 55 to 300 °C was set for the column over a total of 25 min (heating rate: 9.8 °C/min). Qualitative analysis was performed by comparing the mass spectra with those of the NIST 20 library.

HPLC. The fractions obtained were characterized with a Waters ACQUITY HPLC system coupled to a single ESI-MS quadrupole (Waters ZQ Detector, Waters Milford, MA, USA). The analytical column used for the measurements was BIOshell A160 (10 cm × 3.0 mm × 2.7 μm) (Sigma-Aldrich, St. Louis, MO, USA) at a temperature of 35 °C and flow 0.6 mL/min with eluents A (0.1% TFA in H_2O) and B (0.1% TFA in ACN). The elution gradient was always at a flow of 0.6 mL/min starting from 10% B with a linear increase up to 90% B in 5 min. The column was subsequently cleaned with 100% B for 2 min and then reconditioned at 10% B for subsequent analysis for 2 min.

NMR. Solid-state NMR spectra were recorded on a Bruker Avance II spectrometer (Bruker Biospin, Faellanden, CH) operating at 700 MHz ^1H Larmor frequency (16.4 T), corresponding to 146 MHz ^{13}C Larmor frequency. The spectrometer is equipped with a 3.2 BVT MAS probehead in double-resonance mode. The spinning rate was regulated to

https://doi.org/10.1021/acsomega.2c04734
ACS Omega 2022, 7, 37757−37763

11111 ± 2 Hz using dry air, and the temperature was set to 280 K. The pulse lengths were 2.5 and 3.5 μs for ^{1}H and ^{13}C, respectively. Cross-polarization[20] was achieved by matching the k = 1 Hartmann−Hahn condition.[21] For the $\{^{1}H\}^{13}C$ HETCOR spectra, the spectral windows for the different nuclei were 60 and 315 ppm for ^{1}H and ^{13}C, respectively. During the ^{1}H magnetization evolution under the chemical shift in the indirect dimension of heteronuclear correlation experiments, a PMLG decoupling sequence was used to suppress ^{1}H−^{1}H dipolar couplings.[22,23] The CP spectrum was denoised through the MCR procedure.[24,25]

TGA. The thermogravimetric analysis of the sample was carried out with an SDT 650 instrument (TA Instruments, New Castle, DE, USA) A sample (5.52 mg) was placed in an alumina pan. Measurement was performed in the temperature range 19−700 °C with a heating rate of 10 °C/min, using nitrogen as the purge gas.

RESULTS AND DISCUSSION

Feedstock Characterization. An FTIR analysis was performed on a foam fragment. The infrared spectrum (Figure S2, Supporting Information) shows the characteristic absorption bands of an aromatic polyurethane. In particular, the N−H stretching band is visible at 3309 cm^{-1}, and the absorption bands associated with aromatic and aliphatic C−H stretching are observed at around 3000 cm^{-1}. The absorption band at 1710 cm^{-1} is attributable to C═O stretching and the absorption band at 1517 cm^{-1} to C═C stretching. Finally, in the "fingerprint region", absorption related to ester C−O stretching at 1218 cm^{-1} and C−N stretching at 1097 cm^{-1} are observed.[26] Both one- and two-dimensional solid-state ^{13}C NMR spectra were acquired on the sample (Figure 1).

Although broad peaks are usually found for amorphous materials,[27−29] the spectra of the feedstock can be interpreted as compatible with methylene diphenyl diisocyanate linked by 2-methylpropane-(1,3)-diol.

The signals corresponding to aromatic rings (around 130−140 ppm in the ^{13}C dimension) are coupled to methylene protons at around 2.4 ppm, compatible with the structure of the MDI.[35] Two methyl peaks (around 20 ppm in the ^{13}C dimension) of different intensity are present; therefore, we can infer that the polyol linked to 4,4′-MDI contains a methyl group, compatible with the structure of a 2-methylpropane-1,3-diol. The doubling of the methyl peak, with markedly different intensity, could be due again to cross-linking as well as to two different orientations in the link with MDI.

Glycol and aromatics show a mutual interaction and the peaks are quite broad, in agreement with cross-linking. This information allowed us to hypothesize the possible polymeric structure shown in Figure 2.

Finally, a thermogravimetric analysis was performed on the sample. The first derivative curve (Figure S3, Supporting Information) shows the following degradation steps, in agreement with the literature:[30,31] step 1, from 100 to 260 °C, weight loss of 5% due to water evaporation and other small molecules; step 2, from 260 to 350 °C, 40% weight loss due to the breaking of the urethane bonds with the formation of isocyanate and polyol, respectively; step 3, from 350 to 550 °C, 30% weight loss due to decomposition of ester groups.

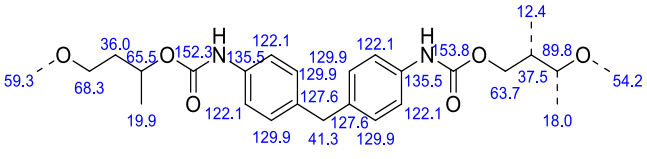

Figure 2. Structure hypothesized for PU.

Enzymatic Digestion. The selected lipase extracted from *Candida rugosa* was not effective in digesting polyurethane foam in fragments. No evidence of enzymatic digestion was detected after 1 week by either LC-MS or GC-MS (Figure 3, top). In contrast, the polyurethane powder was partially attacked by lipase. In the spectra, a partial fragmentation due to the enzymatic digestion process can be observed, as shown in the spectrum second from the top in Figure 3.

HTL Product Yields. The yields of the hydrothermal liquefaction pretreatment, performed as previously described, are shown in Figure 4. It is evident that the process carried out by adding KOH increases the yield in WSO and drastically reduces char formation, as reported in the literature.[16]

Oil Characterization. For the purposes of this study, only organic phases were examined, as they contain oligomers that can be subject to enzymatic degradation. A GC-MS analysis was carried out to determine whether chemicals of industrial interest were present in the oil. In the case of ID1 the analysis revealed the presence of variously substituted quinolines, such as 3-methylquinoline, 3-ethylquinoline, dihydrofuro(2,3-*b*)-quinoline and 8-methyldihydrofuro(2,3-*b*)quinoline. Quinolines are widely used in the production of synthetic dyes and have a high industrial value.[32] 3-Methylpyridine and *o*-toluidine have also been identified. In the case of ID2, carried out in the presence of KOH, two compounds are predominantly formed: 4,4′-methylenedianiline and 3,3′-methylenedianiline. The basic catalyst inhibits the formation of heavy and tarry compounds (TAR), including the quinolines mentioned above. 4,4′-Methylenedianiline is the main precursor for the synthesis of 4,4′-MDI,[33] the most widely used isocyanate for the synthesis of polyurethanes. In both organic fractions, a GC-MS analysis shows the presence of cyclosiloxanes, typical silicone-based surfactants, responsible for the difficult enzymatic degradation of polyurethane foam, making the surface hydrophobic. These silicon-based surfactants prevent cell coalescence through their ability to lower surface tension.[34]

Enzymatic Digestion of Organic Fraction. Enzymatic digestion was carried out on the HTL-pretreated PU under the same conditions as described above. The organic fractions (OP1, OP2) were dried by methanol, since the enzymatic activity decreases in organic solvents. For the organic fraction from ID2, the pH was brought to 7.2 by adding a 1 M HCl solution.

HPLC analysis coupled with both UV and MS was performed on both digested fractions. Comparing the UV spectra of the pretreated digests (OP1D, OP2D) with those obtained from the analysis of OP1 and OP2 shows an increase in the intensity of some signals compared to others (Figure 5). According to the Lambert−Beer law, the intensity of the signals is directly proportional to the concentration of the species in solution. This involves an increase in the concentration of some of the degradation products.

What is remarkable in these spectra is that some signals decrease much more rapidly than others, in some cases up to complete disappearance. From the TIC analysis, it was possible to trace the base peak of the signals labeled below.

https://doi.org/10.1021/acsomega.2c04734
ACS Omega 2022, 7, 37757−37763

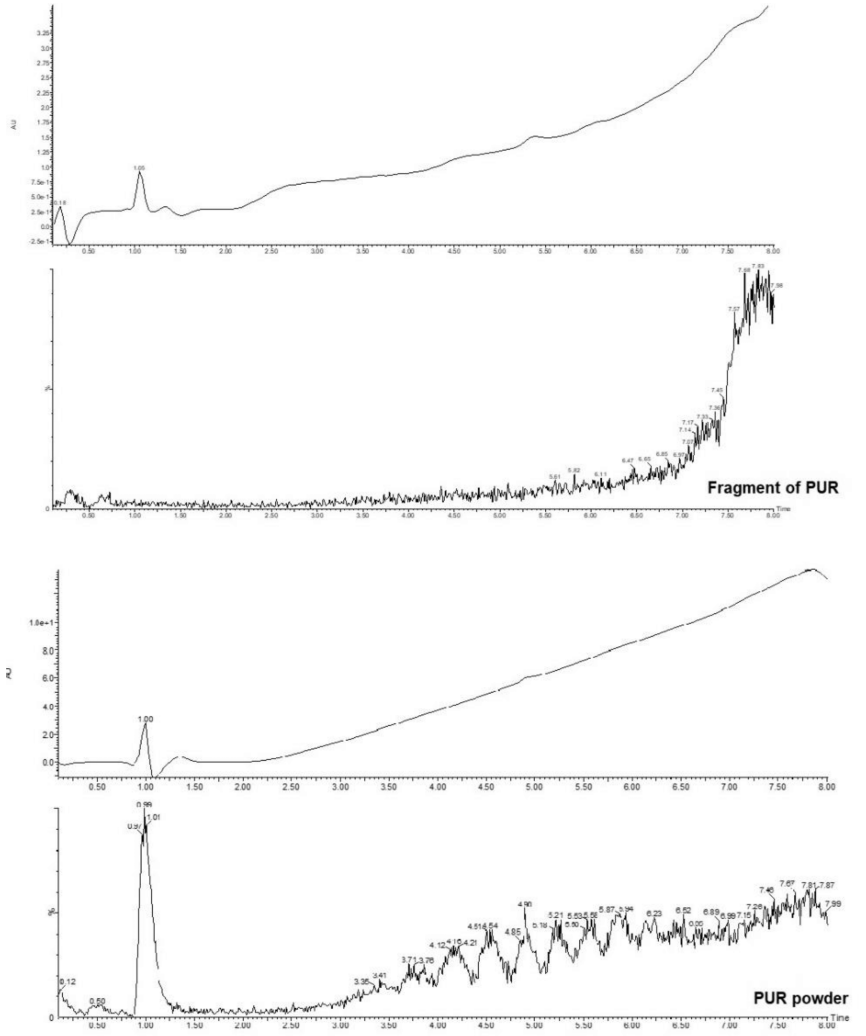

Figure 3. UV−vis and TIC spectra of the digested feedstock.

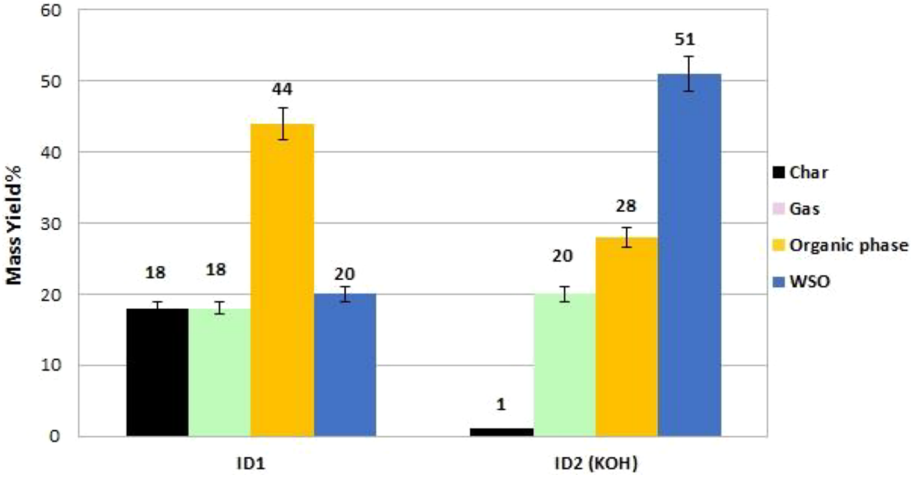

Figure 4. Yields of ID1 and ID2.

OP1D: A, 158.11 *m*/*z*; B, 172.16 *m*/*z*; C, 186.20 *m*/*z*; D, 212.23 *m*/*z*.

OP2D. A, 199.12 *m*/*z*.

These peaks correspond to those identified in the pretreated samples (Figure 5).

CONCLUSIONS

In this preliminary study, we demonstrate for the first time that hydrothermal liquefaction is an effective pretreatment of rigid polyurethane foams to enable an enzymatic digestion. The enzymatic digestion does not occur on the polyurethane bulk and is difficult to achieve on the powdered material, because it

https://doi.org/10.1021/acsomega.2c04734
ACS Omega 2022, 7, 37757−37763

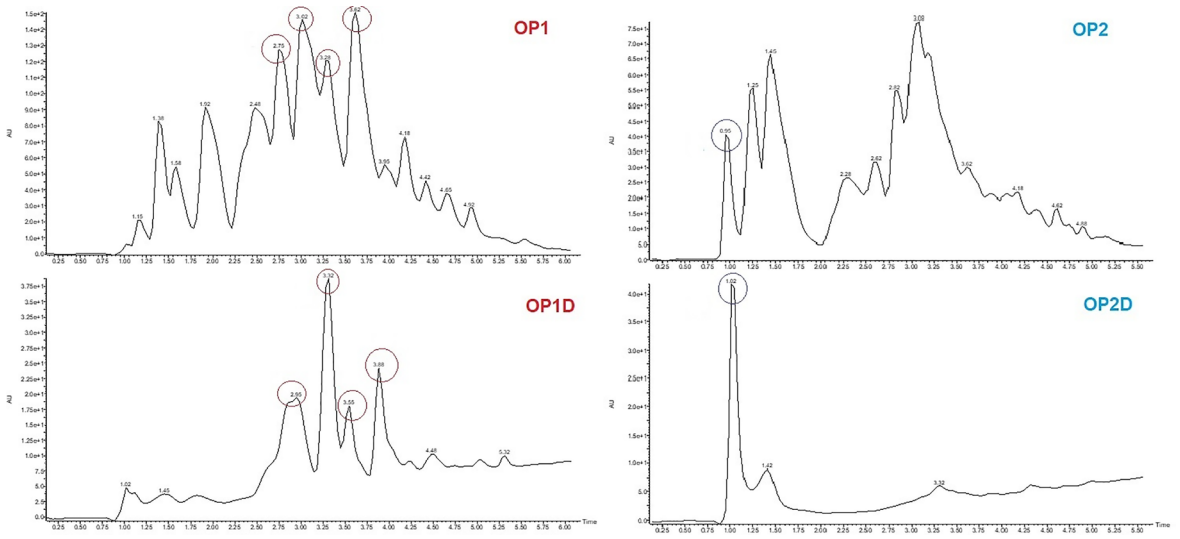

Figure 5. Comparison of UV−vis spectra of HTL organic products (OP1, OP2) and of the digested organic phase (OP1D, OP2D).

occurs at the interface between the enzyme-containing solution and the insoluble plastic material and is further hindered by the presence of apolar surfactants at the surface that prevent the lipase from reaching the surface of the polymer and carrying out efficient digestion. Thanks to the hydrothermal liquefaction pretreatment, the polymer is fragmented into oligomers that end up in the organic phase. Being in the same phase as the enzyme, those are more easily attacked. Enzymatic digestion increases the amount of chemicals by degrading the oligomers formed as a result of the hydrothermal liquefaction treatment. In this work we prove that HTL treatment under subcritical conditions, carried out for relatively short times (20 min), can be an effective method for the enzyme-based enhancement of polyurethanes. With this paper we provide convincing evidence that the combination of HTL and enzymatic digestion is a solid ground on which to develop an alternative to traditional mechanical recycling methods, with the possibility of recovering relevant precursors for the chemical industry (variously substituted quinolines and 4,4′-methylenedianiline) with an outlook of a circular economy.

■ ASSOCIATED CONTENT

Supporting Information

The Supporting Information is available free of charge at https://pubs.acs.org/doi/10.1021/acsomega.2c04734.

Physical−chemical properties of sub- and supercritical water, FT-IR of the rigid polyurethane foam, and TGA and DTG of the rigid polyurethane (PDF)

■ AUTHOR INFORMATION

Corresponding Author

Luca Rosi − *Department of Chemistry "Ugo Schiff", University of Florence, I-50019 Sesto Fiorentino, Italy;* orcid.org/0000-0002-9831-052X; Phone: +055 4573458; Email: luca.rosi@unifi.it

Authors

Riccardo Gallorini − *Department of Chemistry "Ugo Schiff", University of Florence, I-50019 Sesto Fiorentino, Italy;* orcid.org/0000-0003-4535-5502

Benedetta Ciuffi − *Department of Chemistry "Ugo Schiff", University of Florence, I-50019 Sesto Fiorentino, Italy;* orcid.org/0000-0001-9557-5795

Feliciana Real Fernández − *CNR − Istituto di Chimica dei Composti Organometallici (CNR-ICCOM), I-50019 Sesto Fiorentino, Italy; Interdepartmental Research Unit of Peptide and Protein Chemistry and Biology (PeptLab), University of Florence, I-50019 Sesto Fiorentino, Italy; MoD&LS Laboratory, University of Florence, Centre of Competences RISE, I-50019 Sesto Fiorentino, Italy;* orcid.org/0000-0001-5747-2285

Cosimo Carozzini − *Department of Chemistry "Ugo Schiff", University of Florence, I-50019 Sesto Fiorentino, Italy*

Enrico Ravera − *Department of Chemistry "Ugo Schiff", University of Florence, I-50019 Sesto Fiorentino, Italy; Magnetic Resonance Center (CERM), University of Florence, I-50019 Sesto Fiorentino, Italy; Consorzio Interuniversitario Risonanze Magnetiche di Metalloproteine, I-50019 Sesto Fiorentino, Italy;* orcid.org/0000-0001-7708-9208

Anna Maria Papini − *Department of Chemistry "Ugo Schiff", University of Florence, I-50019 Sesto Fiorentino, Italy; Interdepartmental Research Unit of Peptide and Protein Chemistry and Biology (PeptLab), University of Florence, I-50019 Sesto Fiorentino, Italy; MoD&LS Laboratory, University of Florence, Centre of Competences RISE, I-50019 Sesto Fiorentino, Italy;* orcid.org/0000-0002-2947-7107

Complete contact information is available at: https://pubs.acs.org/10.1021/acsomega.2c04734

Author Contributions

Conceptualization: L.R. Methodology: L.R., A.M.P. Formal analysis: R.G., B.C., F.R F. Investigation: B.C., C.C., F.R.F., E.R. Data curation: B.C., R.G., E.R., F.R.F. Writing—original draft preparation: R.G., B.C. Writing—review and editing: E.R., F.R.F., A.M.P., C.C., L.R. Supervision: L.R., A.M.P. Project administration: L.R. Resources: L.R. All authors have read and agreed to the published version of the manuscript.

Funding

L.R. received funding from Fondazione Cassa di Risparmio di Firenze Grant 1504 (ENFORCE Project, Ricercatori a Firenze, 2021).

Notes

The authors declare no competing financial interest.

■ ACKNOWLEDGMENTS

R.G., B.C., E.R., A.M.P., and L.R. wish to thank the Fondazione Cassa di Risparmio di Firenze for financial support (ENFORCE Project, Ricercatori a Firenze, 2021). The authors acknowledge the support and the use of resources of Instruct-ERIC, a landmark ESFRI project, and specifically the CERM/CIRMMP Italy center, as well as of PeptLab and MoD&LS facilities.

■ REFERENCES

(1) Ellen Macarthur Foundation, 2016. The new plastics economy: rethinking the future of plastics. World Economic Forum. https://ellenmacarthurfoundation.org/the-new-plastics-economy-rethinking-the-future-of-plastics (accessed June 7, 2022).
(2) PlasticsEurope.2021. https://plasticseurope.org/knowledge-hub/plastics-the-facts-2021 (accessed July 6, 2022).
(3) Kemona, A.; Piotrowska, M. Polyurethane Recycling and Disposal: Methods and Prospects. *Polymers* **2020**, *12*, 1752.
(4) ISOPA, Fact sheet. Recycling and recovery polyurethanes. Rebonded Flexible Foam, https://www.isopa.org/media/2606/flexible-rebonded-foam.pdf (accessed March 18, 2022).
(5) Zia, K. M.; Bhatti, H. N.; Bhatti, L. A. Methods for polyurethane and polyurethane composites, recycling and recovery: A review. *React. Funct. Polym.* **2007**, *67*, 675−692.
(6) Wei, R.; Zimmermann, W. Microbial enzymes for the recycling of recalcitrant petroleum-based plastics: how far are we? *Microb. Biotechnol.* **2017**, *10*, 1308−1322.
(7) Howard, G. T. Biodegradation of polyurethane: a review. *Int. Biodeterior. Biodegradation.* **2002**, *49*, 245−252.
(8) Yang, L.; Yan, H.; Li, D.; Li, Y.; Zhao, Z. Study on the Properties of Silicon-Modified Polyurethane Anticorrosion Coating. *Chem. Eng. Trans.* **2017**, *59*, 103−108.
(9) Liu, J.; He, J.; Xue, R.; Xu, B.; Qian, X.; Xin, F.; Blank, L. M.; Zhou, J.; Wei, R.; Dong, W.; Jiang, M. Biodegradation and up-cycling of polyurethanes: Progress, challenges, and prospects. *Biotechnol. Adv.* **2021**, *48*, 107730.
(10) Urgun-Demirtas, M.; Singh, D.; Pagilla, K. Laboratory investigation of biodegradability of a polyurethane foam under anaerobic conditions. *Polym. Degrad. Stab.* **2007**, *92*, 1599−1610.
(11) Jansen, B.; Schumacher-Perdreau, F.; Peters, G.; Pulverer, G. Evidence for degradation of synthetic polyurethanes by Staphylococcus epidermidis. *Zentralbl Bakteriol.* **1991**, *276*, 36−45.
(12) Khan, S.; Nadir, S.; Shah, Z. U.; Shah, A. A.; Karunarathna, S. C.; Xu, J.; Jhan, A.; Munir, S.; Hasan, F. Biodegradation of polyester polyurethane by Aspergillus tubingensis. *Environ. Pollut.* **2017**, *225*, 469−480.
(13) Durak, H.; Genel, Y. Hydrothermal conversion of biomass (Xanthium strumarium) to energetic materials and comparison with other thermochemical methods. *J. Supercrit. Fluids.* **2018**, *140*, 290−301.
(14) Castello, D.; Pedersen, T. H.; Rosendahl, L. A. Continuous hydrothermal liquefaction of biomass: A critical review. *Energies* **2018**, *11*, 3165.
(15) Helmer Pedersen, T.; Conti, F. Improving the circular economy via hydrothermal processing of high-density waste plastics. *J. Waste Manag.* **2017**, *68*, 24−31.
(16) dos Passos, J. S.; Glasius, M.; Biller, P. Screening of common synthetic polymers for depolymerization by subcritical hydrothermal liquefaction. *Process Saf. Environ. Prot.* **2020**, *139*, 371−379.
(17) Ciuffi, B.; Loppi, M.; Rizzo, A. M.; Chiaramonti, D.; Rosi, L. Towards a better understanding of the HTL process of lignin-rich feedstock. *Sci. Rep.* **2021**, *11*, 1−9.
(18) Toor, S. S.; Rosendahl, L.; Rudolf, A. Hydrothermal liquefaction of biomass: a review of subcritical water technologies. *Energy* **2011**, *36*, 2328−2342.
(19) Thirunavukarasu, K.; Purushothaman, S.; Gowthaman, M. K.; Nakajima-Kambe, T.; Rose, C.; Kamini, N. R. Utilization of fish meal and fish oil for production of Cryptococcus sp. MTCC 5455 lipase and hydrolysis of polyurethane thereof. *J. Food Sci. Technol.* **2015**, *52*, 5772−5780.
(20) Pines, A.; Gibby, M. G.; Waugh, J. S. Proton enhanced nuclear induction spectroscopy. a method for high resolution NMR of dilute spins in solids. *J. Chem. Phys.* **1972**, *56*, 1776.
(21) Marks, D.; Vega, S. A Theory for Cross-Polarization NMR of Nonspinning and Spinning Samples. *J. Magn. Reson. Series A* **1996**, *118*, 157−172.
(22) Vinogradov, E.; Madhu, P. K.; Vega, S. Proton spectroscopy in solid state nuclear magnetic resonance with windowed phase modulate Lee−Goldburg decoupling sequences. *Chem. Phys. Lett.* **2002**, *354*, 193−202.
(23) Leskes, M.; Singh, T. R.; Madhu, P. K.; Narayanan, D. K.; Shimon, V. Bimodal Floquet description of heteronuclear dipolar decoupling in solidstate nuclear magnetic resonance. *J. Chem. Phys.* **2007**, *127*, 024501.
(24) Tauler, R. Multivariate curve resolution applied to second order data. *Chemom. Intell. Lab. Syst.* **1995**, *30*, 133−146.
(25) Bruno, F.; Francischello, R.; Bellomo, G.; Gigli, L.; Flori, A.; Menichetti, L.; Tenori, L.; Luchinat, L.; Ravera, E. Multivariate Curve Resolution for 2D Solid-State NMR spectra. *Anal. Chem.* **2020**, *92*, 4451−4458.
(26) Vitkauskiene, I.; Makuska, R.; Stirna, U.; Cabulis, U. Synthesis and physical− mechanical properties of polyurethane− polyisocyanurate foams based on PET-waste derived modified polyols. *J. Cell. Plast.* **2011**, *47*, 467−482.
(27) Lin, C.-L.; Kao, H.-M.; Wu, R.-R.; Kuo, P.-N. Multinuclear Solid-State NMR, DSC, and Conductivity Studies of Solid Polymer Electrolytes Based on Polyurethane/Poly(dimethylsiloxane) Segmented Copolymers. *Macromolecules* **2002**, *35*, 3083−3096.
(28) Asakura, T.; Ibe, Y.; Jono, T.; Naito, A. Structure and dynamics of biodegradable polyurethane-silk fibroin composite materials in the dry and hydrated states studied using ^{13}C solid-state NMR spectroscopy. *Polym. Degrad. Stab.* **2021**, *190*, 109645.
(29) Schmidt-Rohr, K.; Spiess, H. In *Multidimensional Solid-State NMR and Polymers*, 1st ed.; Elsevier. 1994; pp 236−276.
(30) Trovati, G.; Sanches, E. A.; Neto, S. C.; Mascarenhas, Y. P.; Chierice, G. O. Characterization of Polyurethane Resins by FTIR, TGA, and XRD. *J. Appl. Polym. Sci.* **2010**, *115*, 263−268.
(31) Reinerte, S.; Kirpluks, M.; Cabulis, U. Thermal degradation of highly crosslinked rigid PU-PIR foams based on high functionality tall oil polyol. *Polym. Degrad. Stab.* **2019**, *167*, 50−57.
(32) Collin, G.; Höke, H.Quinoline and Isoquinoline. In *Ullmann's Encyclopedia of Industrial Chemistry*; Wiley-VCH: 2000; pp 1−5. DOI: 10.1002/14356007.A22_465.
(33) ECHA, 2008. Data on manufacture, import, export, uses and releases of 4,4′-diaminodiphenylmethane as well as information on potential alternatives to its use"; https://echa/2008/02/sr5/eca.227.
(34) Han, M. S.; Choi, S. J.; Kim, J. M.; Kim, Y. H.; Kim, W. N.; Lee, H. S.; Sung, J. Y. Effects of Silicone Surfactant on the Cell Size and Thermal Conductivity of Rigid Polyurethane Foams by Environmentally Friendly Blowing Agent. *Macromol. Res.* **2009**, *17*, 44−50.
(35) Solid-state NMR correlation spectra are based on dipolar rather than on scalar interactions; therefore, we report on spatial and not on through-bond proximities.

https://doi.org/10.1021/acsomega.2c04734
ACS Omega 2022, 7, 37757−37763